Doctoral Dissertation (Censored)
博士論文 (要約)

Study of muonic X-ray spectroscopy and nuclear muon capture reaction

(ミューオン原子 X 線分光と原子核ミューオン捕獲反応の研究)

A Dissertation Submitted for the Degree of Doctor of Philosophy
December 2021

令和 3 年 12 月博士(理学)申請

Department of Physics, Graduate School of Science,
The University of Tokyo

東京大学理学系研究科物理学専攻

Takeshi Y. Saito
齋藤岳志

Abstract

A negative muon forms an atomic binding state with a nucleus, called a muonic atom. The X ray emitted by the muonic atom is referred to as a muonic X ray. The muonic X ray has been used to measure the nuclear charge radius because the energy of the muonic X ray is sensitive to the charge radius. Due to the increasing attention to nuclear charge distribution, it is important to develop the interpretation method to discuss the charge distribution with the muonic X ray in addition to the radius.

The muonic atom mainly decays via a capture process $p^+ + \mu^- \rightarrow n + \nu_\mu$ and it is called the nuclear muon capture reaction, or simply the muon capture. Since the muon has a large mass, the excited state produced by the muon capture has large excitation energy. However, little is known about the structure of the excited state following the muon capture. The neutrons emitted from the excited state are a probe of the excited state following the muon capture. The experimental study is lacking especially for the medium-heavy region.

The thesis consists of two parts.

In Part I, the muonic X ray spectroscopy is discussed. The analysis method of the muonic X ray to deduce the charge radii and to discuss the charge distribution is described using the experimental data of the muonic X ray from the muonic palladium. The experiment was performed at the RCNP MuSIC-M1 beamline. The energy of the muonic X rays from the muonic palladium with the mass number of $A = 104$, 105, 106, 108, and 110 was measured by germanium detectors. The charge radius of the palladium isotopes is determined by assuming two-parameter Fermi distribution as the charge distribution. It is indicated that the energy of the higher X-ray transitions plays an important role to deduce the model dependence in the interpretation. The charge distribution is discussed using the extended nuclear moment called Barrett moment. The charge distribution obtained from the electron scattering and the theoretical calculation is compared with the present result of the muonic X rays for ^{108}Pd. The necessary precision for the future measurement of the muonic X rays is discussed with the uncertainty of the current experiment.

The subject of Part II is the neutron emission following the muon capture reaction. The measurement of the neutrons emitted following the muon capture on the palladium isotopes with the mass number of $A = 104$, 105, 106, 108, and 110 was performed. The experiments were performed at the RCNP MuSIC-M1 beamline. The neutron energy spectrum was obtained by the time-of-flight method for the 1-20 MeV region. The characteristic spectra with a two-component structure, which consists of the low energy evaporation neutron below 5 MeV and high energy direct component above it, were observed. The spectral shape of the neutron energy is discussed by comparing the previous result for heavier nuclei and theoretical calculation. The neutron-neutron angular correlation was also measured. Excess at the small opening angle is found for the first time. Further experimental and theoretical study is required to reveal the process of deexcitation after the muon capture reaction.

Contents

List of Figures

List of Tables

Chapter §

Introduction

This chapter is an introductory part of the thesis. The general descriptions and motivations for the muon X-ray spectroscopy and neutron spectroscopy are described in Sec. §.1 and §.2, respectively. The objective and outline of the thesis are summarized in Sec. §.3.

§.1 Muonic X-ray spectroscopy

§.1.1 Charge radius of atomic nucleus

The atomic nucleus is a finite quantum many-body system that consists of nucleons, namely protons and neutrons. The size of the nucleus is typically several fm and the size itself is the most direct consequence of the finiteness. The size and shape of the nucleus are thus directly related to the nuclear potential, the single-particle orbit, and wavefunctions[1]. By measuring the size of the nuclei, unique phenomena such as shell evolution[2] and neutron halo[3], have been observed. Moreover, the size of the nucleus is the basement of the precise measurement for particle physics[4].

The size, simply root-mean-square (rms) radius, of the nucleus can be defined in two ways. Corresponding to two nucleons, protons and neutrons, there are two radii of the nucleus; the charge radius and matter radius. The charge radius is the radius that is related to the electromagnetic interaction and the proton distribution dominates the charge radius. The matter radius is that to the nuclear force and both of the protons and neutrons contribute to it. Usually, the charge and matter radii are different and the difference is the subject of the recent experimental and theoretical studies. Therefore the precise determination of both radii is important. In this study, the experimental determination of the charge radius is focused on.

In addition to the rms charge radius, the charge distribution is recently getting attention. The rms radius is the second-order moment of the charge distribution. The higher-order moment, especially the fourth moment $< r^4 >$, is important to determine the surface thickness[5–7]. To obtain the higher moment, the charge distribution should be determined by extending the measurement of the rms radius.

The charge radius has been measured mainly by three experimental methods. The optical isotope shift (OIS) measurement of the electronic atom is the most precise method for the relative value. Because of the difficulty to solve the many-body problem, the OIS measurement cannot determine the absolute value of the radius. The electron scattering experiment and the measurement of the muonic X-ray transition energy are used for the absolute value. The experimental precision of the two methods is almost the same and the systematic uncertainty is different. Thus the electron scattering and muonic X-ray is complementary for the determination of the charge radius[1, 8, 9].

The electron scattering can measure the charge distribution and systematic measurement has been performed for most of the stable nuclei. Furthermore, a recent study is making it possible to perform electron scattering experiments for unstable nuclei[10, 11]. On the other hand, the muonic X-ray transition energy is only used for the determination of the charge radius and there is no discussion of the charge distribution with the muonic X-ray transition energy.

§.1.2 Muonic atom and muonic X ray

The muon is a particle with the mass of 105.6583715 MeV/c^2 and the charge ± 1[12]. There is negative and positive muon and hereafter only the negative muon is discussed since only the negative muon can form the bound state with the positively charged nucleus.

The muonic atom is the bound state of the nucleus and the negative muon. Because of the mass difference, the atomic radius (Bohr radius) of the muonic atom is about 200 times smaller than that of the ordinary electronic atom. The wavefunction and the binding energy of the muonic atom are more sensitive to the nuclear charge distribution than the electronic atom due to the smaller atomic radius. The binding energy of the electronic and muonic atom is also different by about 200 times. Since the spatial and energy scale of the electronic and muonic atom is much different, the surrounding electrons can be neglected and the muonic atom can be considered as a two-body system in the first approximation[13–15]. Furthermore, the dominant interaction between the muon and the nucleus is only the electromagnetic interaction during the formation of the atom. This simple description of the muonic atom makes the theoretical interpretation easier compared to the electronic atom, which is the target of the OIS measurement. Therefore, the nuclear charge radius can be determined by measuring the binding energy of the muonic atom.

The muonic X ray is the transition X ray emitted from the muonic atom. Because the muon is firstly filled at the binding state with a high principal quantum number (typically $n \sim 15$) during the formation of the muonic atom[16], the emission of the muonic X ray usually accompanies the formation of the muonic atom without any managements. The transition energy of the muonic X ray is the difference in the energy of the initial and final states. Thus the measurement of the muonic X rays makes it possible to determine the binding energy of the muonic atom experimentally. The typical energy of the muonic X ray is from several tens keV to several MeV. This energy is suited to be measured by γ-ray detectors, such as semiconductor detectors[17].

The uncertainty of the radius determined by the muonic X ray is contributed by the interpretation in addition to the experimental uncertainty. To interpret the muonic transition energy into the charge radius, the model charge distribution should be assumed for the numerical calculation. As for the most common compilation [9], the two-parameter Fermi distribution with a fixed surface diffuseness is assumed. The model uncertainty of the calculation is not straightforward, and it is difficult to quantitatively evaluate the model dependence.

The higher-order transitions of the muonic X ray provide a new perspective to the interpretation of the muonic transition energy. In the previous studies, only the K_α series ($2p$-$1s$ transitions) are used in the discussion for the charge radius because they have the highest sensitivity to the charge distribution. Several earlier studies[18, 19] report the higher transitions and they actually discuss the detailed aspects of the muonic X-ray transition. On the other hand, the number of the

experimental inputs limits the number of the parameters that can be determined. The higher transition must be included in the analysis to determine the diffuseness parameter in the two-parameter Fermi distribution.

More generally, the charge distribution can be discussed with the higher transition in addition to the charge radius. In this thesis, the model which was introduced by Barrett[20] is extended and a new approach to discuss the charge distribution by the muonic X ray is proposed. In this approach, the muonic transition energy is quantitatively compared with the charge distribution which is deduced from the theory and the electron scattering experiment.

The palladium isotope ($Z = 46$) is used as the target nuclei. In this study, the muonic X rays of the stable palladium isotopes with $A = 104$, 105, 106, 108, and 110 were measured. The lowest $2p$-$1s$ transition energy is already measured and summarized in the compilation [9] and the charge radii are also tabled in it. As discussed above, in this compilation, the charge radii are deduced with only the lowest transitions and the uncertainty estimation is not performed for the rms radii. Moreover, the original paper is not published for several nuclei in the compilation including the palladium isotopes. This situation makes it difficult to ensure the credibility of the charge radius, which is one of the most fundamental parameters in natural science.

§.2 Neutron emission following nuclear muon capture

The atomic ground state of a muonic atom decays via two weak processes[21]. One is μ-e decay as same as the bare muon in the vacuum;

$$\mu^- \rightarrow e^- + \bar{\nu_e} + \nu_\mu. \tag{§.1}$$

The other is the nuclear muon capture reaction. The nuclear muon capture reaction (hereafter, merely muon capture) is the process in which a proton in the nucleus captures the negative muon and transforms into a neutron. The elementary process is described as

$$\mu^- + p^+ \rightarrow n + \nu_\mu. \tag{§.2}$$

The branching ratio depends on the nuclei. For the light nuclei such as hydrogen or carbon, the muonic atom decays via μ-e decay. The probability of the muon capture, namely the lifetime of the muonic atom, roughly depends on the fourth of the nuclear charge Z^4[22]. Except for the lightest nuclei, the muon capture is the dominant process and more than 90% of the muonic atom decays via the muon capture[23].

The elementary process of the muon capture is similar to the electron capture

$$e^- + p^+ \rightarrow n + \nu_e. \tag{§.3}$$

The largest difference is the mass of the capturing lepton. The muon has the mass of 105.6 MeV/c^2 and the absence of the muon after the reaction of the muon capture (§.2) makes the Q value of the reaction large $\sim$ 100 MeV. Because of the large Q value, which is larger than the typical Fermi energy of the nucleus, all nuclei can decay via the muon capture reaction suppose the muon is there.

For the nucleus with (Z,A), the muon capture remains the excited state of ($Z-1$,A) nucleus as

$$\mu^- + (Z, A) \rightarrow (Z-1, A)^* + \nu_\mu. \tag{§.4}$$

The large Q value provides the high excitation energy for the nucleus. While a large part of the energy is taken away by the kinetic energy of the emitting neutrino, the typical excitation energy is from several MeV to several tens MeV. Due to the large excitation energy, the residual nuclei usually deexcites by emitting neutrons, γ rays, and sometimes light charged particles. Contrary to the simple description of the elementary process, little is known about the excited state following the muon capture. Since the neutrino is difficult to detect by the ordinary detector, even the excitation function has not been directly measured[21].

The particles emitted from the excited state following the muon capture are the possible clue for the excitation structure of the muon capture. Except for the γ rays, the neutrons are the major part of the emitted particles because the charged particle emission such as protons and deuterons is hindered by the Coulomb barrier. The charged particle emission is the order of 1% for medium-heavy nuclei for example[21, 24]. The typical number distribution of the emitted neutrons is illustrated in Fig. §.1. The largest path of the decay process is the one neutron emission whereas approximately half of the muon capture reaction is accompanied by multi neutron emission[21, 25, 26].

The energy spectrum of the emitted neutrons is a fundamental aspect of the decay process of the muon capture. The previous study by Schröder measured the neutron energy for thallium, lead, and bismuth. The measured neutron energy spectra shown in Fig. §.2 contain two components; the low energy neutrons below 5 MeV and the high energy neutrons above it. The low energy component is interpreted as the evaporation neutron from the highly excited nucleus. The high-energy neutron is the direct neutron, which is the neutron that is kicked by the elementary process (§.2) out of the nucleus with fewer scatterings to the other nucleons[27].

The high-energy neutrons have been investigated for several nuclear species[21, 28–30]. It is revealed that the high energy component continues up to 100 MeV, which is the possible maximum energy of the muon capture reaction. On the other hand, the low energy neutrons below 5 MeV have not been paid much attention. In addition to the Schröder's result for three heavy nuclei, a few results are reported for light nuclei such as carbon and oxygen[31, 32]. However, there is no direct measurement of the neutron energy for the medium-heavy region $A \sim 100$. Furthermore, these previous studies use the natural target and the isotope dependence of the neutron energy has not been discussed.

The palladium is the medium-heavy $Z = 46$ nuclei with six stable isotopes. In this study, the neutron energy following the muon capture on the palladium isotope enriched target with $A =$ 104,105, 106, 108, and 110 are measured experimentally.

In addition to the energy spectrum of the neutrons, the angular correlation of the neutrons is considered to reflect the microscopic structure of the excited state after the muon capture. There is one previous study to measure the angular correlation of the neutron following the muon capture for ^{40}Ca[28]. They reported the excess at a large opening angle with high energy neutron with the energy deposit above 10 MeV as shown in Fig. §.3. On the other hand, the neutron-neutron correlation has not been measured for the low-energy neutrons. Therefore, the coincidence measurement would provide new information for the muon capture reaction.

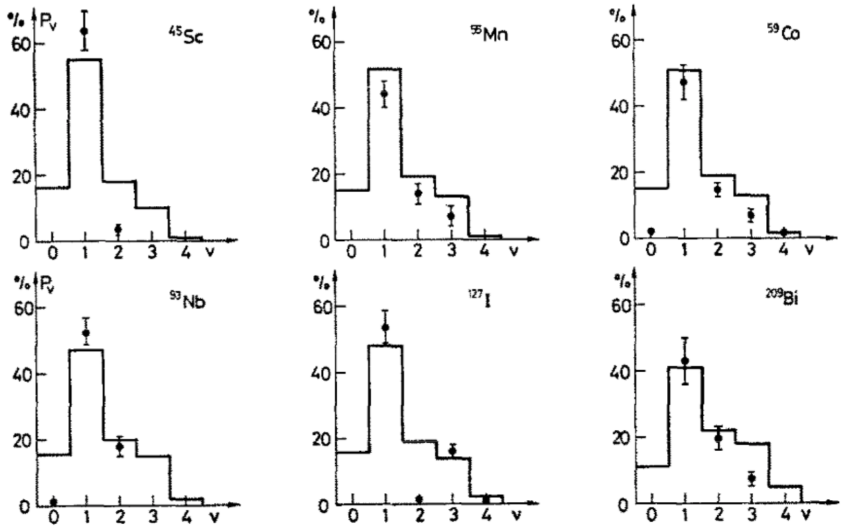

FIGURE §.1: Neutron multiplicity of several nuclei. The points indicate the experimental results and the lines are theoretical predictions. The figure is taken from [25].

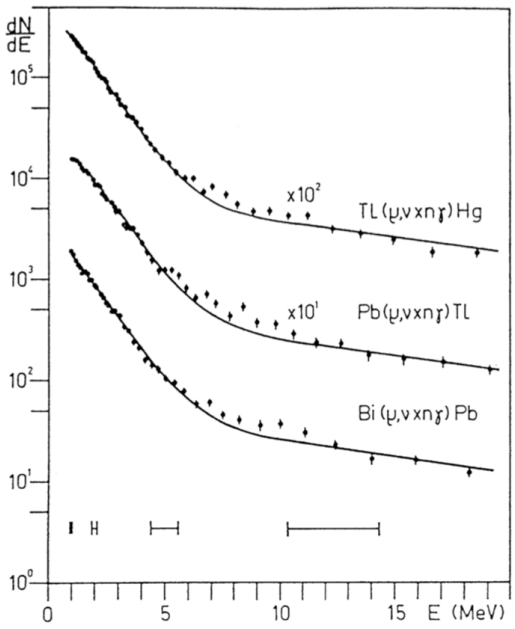

FIGURE §.2: Neutron energy spectrum for Tl, Pb, ad Bi. The points are the experimental results and the vertical error bars indicate the energy uncertainty. There is a kinked structure around 5 MeV. The figure is taken from [33].

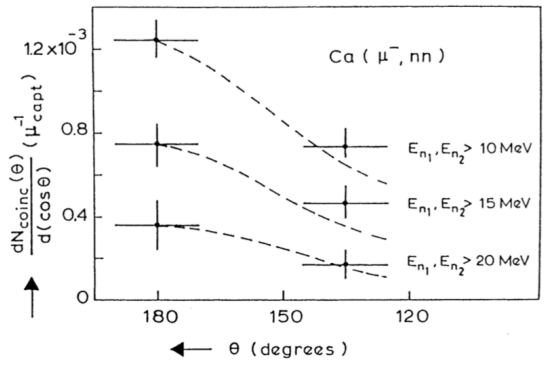

FIGURE §.3: Neutron angular correlation for ^{40}Ca. The results are illustrated for several neutron energy thresholds. The figure is taken from [28]

§.3 Thesis objective and outline

The thesis consists of two parts; the muonic X ray spectroscopy (Part I) and neutron emission following the nuclear muon capture (Part II).

The objectives of Part I of the thesis is three points:

- Summarize the experimental and analysis method to measure the experimental value of the muonic X ray transition energy.
- Give the experimental result of muonic transition energy and the determined charge radii for the stable palladium isotopes.
- Propose a new method to interpret the experimental data to nuclear charge distribution.
- Suggest the necessary experimental resolution for the future experiment.

Part I consists of four chapters. The experimental setup to measure muonic X ray of the palladium isotopes is described in Chap. I-1 and the analysis of the experimental data is in Chap. I-2. The result of the analysis, namely the measured transition energy, is summarized and the charge radius and charge distribution are discussed using the result in Chap. I-3. In Chap. I-4, the conclusion and future outlook are described.

The objectives of Part II is :

- Measure the neutron energy following the muon capture on stable palladium isotopes with the mass number of 104, 105, 106, 108, and 110 for the low-energy region below 20 MeV.
- Measure the neutron angular correlation for these isotopes.
- Compare them with the previous measurement and the theoretical calculation.

Part II consists of four chapters. The experimental setup including the beamline, target, and detector system is described in Chap. II-1 while some of the experimental setups are common with Part I. The analysis to deduce the neutron energy and angular correlation is written in Chap. II-2. The resulted spectrum is summarized in Chap. II-3. In this chapter, a comparison of the experimental result with the

previous experiment and the theoretical calculation is discussed. Chapter II-4 is for the summary and future outlook.

For the experimental works in the thesis, the author has contributed to

- Design of the detector setup (Part I, II)
- Development the data acquisition system (Part I, II)
- Planing of the beamtime schedule (Part I, II)
- Data analysis to determine the transition energy (Part I) and the neutron energy spectrum and the angular correlation (Part II)
- Development of the numerical calculation code for the muonic transition energy (Part I)
- Development of the interpretation method of the muonic X ray to the charge radii and distribution (Part I)
- Major part of the discussion (Part II).

Part I

Muonic X-ray spectroscopy

Part I

本 Part については、5 年以内に雑誌等で刊行予定のため、非公開。

Part II

Neutron emission following nuclear muon capture

Part II

本 Part については、5 年以内に雑誌等で刊行予定のため、非公開。

Appendix A

本 Appendix については、5 年以内に雑誌等で刊行予定のため、非公開。

Acknowledgements

I am deeply grateful to the people who have supported me during my five years in the Ph.D. course. This work could not have been completed without their help and guidance.

First and foremost, I would like to express my special appreciation to my supervisor, Prof. H. Sakurai. He continuously supported me throughout my research with his broad knowledge of nuclear and related physics, strict way of thinking scientifically, and warm encouragement. He also gave me a lot of opportunities to participate in a variety of the experimental projects both in Japan and abroad.

My sincere gratitude also goes to Dr. T. Matsuzaki and Dr. M. Niikura, who are the core collaborators of the thesis work. Dr. T. Matsuzaki always provided lots of precise advice from the viewpoint of an expert scientist. I was helped many times by the practical and kind guidance by Dr. M. Niikura for both experimental works and writing.

I would like to thank all the collaborators who participated in the experiments; Dr. M. Igashira, Dr. K. Imao, Dr. K. Ishida, Dr. R. Katabuchi, Dr. S. Kawase, Dr. Y. Kawashima, Dr. T. Koiwai, Dr. M. K. Kubo, Mr. K. Matsui, Dr. Y. Miyake, Dr. S. Momiyama, Dr. Y. Mori, Mr. A. Nambu, Dr. K. Ninomiya, Dr. H. Otsu, Dr. A. Sato, Dr. K. Shimomura, Dr. P. Strasser, Dr. X. Sun, Dr. A. Taniguchi, Dr. D. Tomono, Dr. H. Wang, Dr. Y. Watanave, and Dr. K. Wimmer. The beamtimes were tough and could not have been happily finished literally without anyone.

I would like to thank the theoreticians, Dr. T. Naito, Dr. F. Minato, and Dr. S. Abe, who provided many helpful discussions and calculations for the thesis work. Dr. T. Naito and Dr. F. Minato had a meaningful discussion for the numerical calculation in Part I. Dr. S. Abe provided the theoretical calculations, which were crucial for the discussion in Part II.

I appreciate all the members of the nuclear physics experiment (NEX) group at the University of Tokyo, Prof. Dr. Sakurai, Prof. Dr. R. S. Hayano, Dr. K. Wimmer, Dr. T. Suzuki, Dr. M. Niikura, Dr. R. Taniuchi, Mr. K. Matui, Dr. Y. Murakami, Mr. H. Yamada, Dr. S. Momiyama, Dr. Y. Watanabe, Dr. S. Koyama, Mr. S. Nagamine, Mr. T. Ando, Dr. T. Koiwai, Mr. T. Aoki, Mr. K. Kokubun, Ms. R. Mizuno, Mr. S. Yamamura, and Mr. T. T. Yeung (Marco). I have really enjoyed the daily conversations and fruitful discussions, even though I did not directly collaborate with all of them. My only regret is that we could not have so many offline talks for the recent two years due to the COVID-19 situation.

I would like to express my gratitude to the thesis reviewers, Prof. Dr. K. Yako, Prof. Dr. Y. Fukushima, Prof. Dr. T. Mori, Prof. Dr. K. Ozawa, Prof. Dr. H. Liang for their many valuable comments and discussions for the thesis.

Last but not least, I would like to say thank you to my parents, friends, and partner for their continuous support and encouragement.

Bibliography

1. Ozawa, A., Suzuki, T. & Tanihata, I. Nuclear size and related topics. *Nuclear Physics A* **693.** Radioactive Nuclear Beams, 32–62. ISSN: 0375-9474. https://www.sciencedirect.com/science/article/pii/S0375947401011526 (2001).
2. Bissell, M. L. *et al.* Cu charge radii reveal a weak sub-shell effect at $N = 40$. *Phys. Rev. C* **93,** 064318. https://link.aps.org/doi/10.1103/PhysRevC.93.064318 (6 2016).
3. Tanihata, I. Neutron halo nuclei. *Journal of Physics G: Nuclear and Particle Physics* **22,** 157–198. https://doi.org/10.1088/0954-3899/22/2/004 (1996).
4. Reinhard, P.-G. & Nazarewicz, W. Nuclear charge densities in spherical and deformed nuclei: Toward precise calculations of charge radii. *Phys. Rev. C* **103,** 054310. https://link.aps.org/doi/10.1103/PhysRevC.103.054310 (5 2021).
5. Reinhard, P.-G., Nazarewicz, W. & Garcia Ruiz, R. F. Beyond the charge radius: The information content of the fourth radial moment. *Phys. Rev. C* **101,** 021301. https://link.aps.org/doi/10.1103/PhysRevC.101.021301 (2 2020).
6. Naito, T., Colò, G., Liang, H. & Roca-Maza, X. Second and fourth moments of the charge density and neutron-skin thickness of atomic nuclei. *Phys. Rev. C* **104,** 024316. https://link.aps.org/doi/10.1103/PhysRevC.104.024316 (2 2021).
7. Kurasawa, H. & Suzuki, T. The nth-order moment of the nuclear charge density and contribution from the neutrons. *Progress of Theoretical and Experimental Physics* **2019.** 113D01. ISSN: 2050-3911. eprint: https://academic.oup.com/ptep/article-pdf/2019/11/113D01/31149972/ptz121.pdf. https://doi.org/10.1093/ptep/ptz121 (Nov. 2019).
8. Angeli, I. & Marinova, K. Table of experimental nuclear ground state charge radii: An update. *Atomic Data and Nuclear Data Tables* **99,** 69 –95. ISSN: 0092-640X. http://www.sciencedirect.com/science/article/pii/S0092640X12000265 (2013).
9. Fricke, G. *et al.* Nuclear Ground State Charge Radii from Electromagnetic Interactions. *Atomic Data and Nuclear Data Tables* **60,** 177 –285. ISSN: 0092-640X. http://www.sciencedirect.com/science/article/pii/S0092640X85710078 (1995).
10. Wakasugi, M. *et al.* Construction of the SCRIT electron scattering facility at the RIKEN RI Beam Factory. *Nucl. Instrum. Meth.* **B317,** 668–673 (2013).
11. Tsukada, K. *et al.* First Elastic Electron Scattering from ^{132}Xe at the SCRIT Facility. *Phys. Rev. Lett.* **118,** 262501. https://link.aps.org/doi/10.1103/PhysRevLett.118.262501 (26 2017).
12. Olive, K. A. *et al.* Review of Particle Physics. *Chin. Phys.* **C38,** 090001 (2014).
13. Schaller, L. A. Muonic atoms spectroscopy. *Zeitschrift für Physik C Particles and Fields* **56,** S48–S58. ISSN: 1431-5858. http://dx.doi.org/10.1007/BF02426775 (1992).

14. Borie, E. & Rinker, G. A. The energy levels of muonic atoms. *Rev. Mod. Phys.* **54,** 67–118. https://link.aps.org/doi/10.1103/RevModPhys.54.67 (1 1982).
15. Sakurai, J. *Advanced quantum mechanics*
16. Kirch, K. *et al.* Muonic cascades in isolated low-Z atoms and molecules. *Phys. Rev. A* **59,** 3375–3385. https://link.aps.org/doi/10.1103/PhysRevA.59.3375 (5 1999).
17. Leo, W. R. *Techniques for Nuclear and Particle Physics Experiments*
18. Barreau, P., Roussel, L. & Powers, R. A muonic X-ray study of the charge distribution of 147Sm AND 149Sm. *Nuclear Physics A* **364,** 446–460. ISSN: 0375-9474. https://www.sciencedirect.com/science/article/pii/0375947481905819 (1981).
19. Bergem, P. *et al.* Nuclear polarization and charge moments of ^{208}Pb from muonic x rays. *Phys. Rev. C* **37,** 2821–2833. https://link.aps.org/doi/10.1103/PhysRevC.37.2821 (6 1988).
20. Barrett, R. Model-independent parameters of the nuclear charge distribution from muonic X-rays. *Physics Letters B* **33,** 388 –390. ISSN: 0370-2693. http://www.sciencedirect.com/science/article/pii/0370269370906118 (1970).
21. Measday, D. F. The nuclear physics of muon capture. *Physics Reports* **354,** 243–409. ISSN: 03701573. http://linkinghub.elsevier.com/retrieve/pii/S0370157301000126 (2001).
22. Primakoff, H. Theory of Muon Capture. *Rev. Mod. Phys.* **31,** 802–822. http://link.aps.org/doi/10.1103/RevModPhys.31.802 (3 1959).
23. Suzuki, T., Measday, D. F. & Roalsvig, J. P. Total nuclear capture rates for negative muons. *Physical Review C* **35,** 2212–2224. ISSN: 05562813 (1987).
24. Wyttenbach, A. *et al.* Probabilities of muon induced nuclear reactions involving charged particle emission. *Nuclear Physics A* **294,** 278–292. ISSN: 0375-9474. https://www.sciencedirect.com/science/article/pii/037594747890218X (1978).
25. Backenstoss, G. *et al.* Nuclear γ-rays following muon capture. *Nuclear Physics A* **162,** 541 –551. ISSN: 0375-9474. http://www.sciencedirect.com/science/article/pii/0375947471902533 (1971).
26. Macdonald, B., Diaz, J. A., Kaplan, S. N. & Pyle, R. V. Neutrons from Negative-Muon Capture. *Phys. Rev.* **139,** B1253–B1263. http://link.aps.org/doi/10.1103/PhysRev.139.B1253 (5B 1965).
27. Singer, P. Neutron emission following muon capture in heavy nuclei. *Il Nuovo Cimento* **23,** 669–689. ISSN: 00296341 (1962).
28. Kozlowski, T *et al.* Energy spectra and asymmetries of neutrons emitted after muon capture. *Nucl. Phys. A* **436,** 717–732 (Apr. 1985).
29. Sundelin, R. M. & Edelstein, R. M. Neutron Asymmetries and Energy Spectra from Muon Capture in Si, S, and Ca. *Phys. Rev. C* **7,** 1037–1060. https://link.aps.org/doi/10.1103/PhysRevC.7.1037 (3 1973).
30. McIntyre, E. *et al.* Spectra of gamma rays and energetic neutrons from μ^- capture in 165Ho. *Physics Letters B* **137,** 339–342. ISSN: 0370-2693. https://www.sciencedirect.com/science/article/pii/0370269384917283 (1984).

31. Van Der Schaaf, A. *et al.* Measurement of neutron energy spectra and neutron-gamma angular correlations for the muon capture process 16O(mu^-, ν μxn)14, 15N. *Nuclear Physics A* **408,** 573–589. ISSN: 0375-9474. https://www.sciencedirect.com/science/article/pii/0375947483902464 (1983).

32. Plett, M. E. & Sobottka, S. E. Effects of the Giant Resonance on the Energy Spectra of Neutrons Emitted Following Muon Capture in ^{12}C and ^{16}O. *Phys. Rev. C* **3,** 1003–1010. https://link.aps.org/doi/10.1103/PhysRevC.3.1003 (3 1971).

33. Schröder, W. U. *et al.* Spectra of neutrons from μ capture in thallium, lead and bismuth. *Zeitschrift für Physik* **268,** 57–64. ISSN: 0044-3328. https://doi.org/10.1007/BF01670062 (1974).

34. *Research Center for Nuclear Physics* http://www.rcnp.osaka-u.ac.jp.

35. *A NEW DC MUON BEAM LINE AT RCNP, OSAKA UNIVERSITY* Y. Matsumoto, IPAC16 proceedings (2016).

36. Cook, S. *et al.* Delivering the world's most intense muon beam. *Phys. Rev. Accel. Beams* **20,** 030101. https://link.aps.org/doi/10.1103/PhysRevAccelBeams.20.030101 (3 2017).

37. Terada, K. *et al.* Measurement of neutron capture cross sections of Pd-107 at J-PARC/MLF/ANNRI. *Progress in Nuclear Energy* **82.** Selected Papers from the Fourth International Symposium on Innovative Nuclear Energy Systems, INES-4 - Innovative Nuclear Science and Technology Post Fukushima - held at Ookayama campus of Tokyo Institute of Technology, 118 –121. ISSN: 0149-1970. http://www.sciencedirect.com/science/article/pii/S014919701400198X (2015).

38. Baba, H., Takeuchi, S., Yoneda, K., Shimoura, S. & Ieki, K. Development of New Data Acquisition System BabarlDAQ for Nuclear Physics Experiments. *RIKEN Accel. Prog. Rep.* **34,** 221 (2001).

39. Baba, H. *et al.* New data acquisition system for the RIKEN Radioactive Isotope Beam Factory. *Nuclear Instruments and Methods in Physics Research Section A: Accelerators, Spectrometers, Detectors and Associated Equipment* **616,** 65–68. ISSN: 0168-9002. https://www.sciencedirect.com/science/article/pii/S0168900210003761 (2010).

40. *Mesoroentgen Spectra Catalogue* http://muxrays.jinr.ru/index.html.

41. Barrett, R. C. Nuclear charge distributions. *Reports on Progress in Physics* **37,** 1–54. https://doi.org/10.1088%2F0034-4885%2F37%2F1%2F001 (1974).

42. Michel, N., Oreshkina, N. S. & Keitel, C. H. Theoretical prediction of the fine and hyperfine structure of heavy muonic atoms. *Phys. Rev. A* **96,** 032510. https://link.aps.org/doi/10.1103/PhysRevA.96.032510 (3 2017).

43. *National Nuclear Data Center* http://www.nndc.bnl.gov/chart.

44. Cheng, K. T., Sepp, W. D., Johnson, W. R. & Fricke, B. Self-energy corrections in heavy muonic atoms. *Phys. Rev. A* **17,** 489–492. https://link.aps.org/doi/10.1103/PhysRevA.17.489 (2 1978).

45. Rinker, G. & Speth, J. Nuclear polarization in muonic atoms. *Nuclear Physics A* **306,** 397 –405. ISSN: 0375-9474. http://www.sciencedirect.com/science/article/pii/0375947478904712 (1978).

46. Bohr, A. & Mottelson, B. R. *Nuclear Structure* 1971.

47. Laan, L. B. v. d. Electron scattering of palladium isotopes. *PhD. Thesis, Amsterdam Univ.* (1986).
48. *Interacting Plot of Atomic nuclei and Computed Shapes* https://wwwnucl.ph.tsukuba.ac.jp/InPACS/.
49. Ford, K. W. & Rinker, G. A. Analysis of Muonic- Atom X Rays in the Lead Isotopes. *Phys. Rev. C* **7,** 1206–1221. https://link.aps.org/doi/10.1103/PhysRevC.7.1206 (3 1973).
50. Phan, T. Q., Bergem, P., Rüetschi, A., Schaller, L. A. & Schellenberg, L. Nuclear polarization in muonic ^{90}Zr. *Phys. Rev. C* **32,** 609–619. https://link.aps.org/doi/10.1103/PhysRevC.32.609 (2 1985).
51. Ebata, S., Nakatsukasa, T. & Inakura, T. Systematic investigation of low-lying dipole modes using the canonical-basis time-dependent Hartree-Fock-Bogoliubov theory. *Phys. Rev. C* **90,** 024303. https://link.aps.org/doi/10.1103/PhysRevC.90.024303 (2 2014).
52. Ebata, S. & Nakatsukasa, T. Octupole deformation in the nuclear chart based on the 3D Skyrme Hartree–Fock plus BCS model. *Physica Scripta* **92,** 064005. ISSN: 1402-4896. http://dx.doi.org/10.1088/1402-4896/aa6c4c (2017).
53. Arthur, R. G. *et al.* Vibrational states in108Pd studied by elastic and inelastic electron scattering. *Journal of Physics G: Nuclear Physics* **4,** 961–972. https://doi.org/10.1088/0305-4616/4/6/023 (1978).
54. Sato, T. *et al.* Particle and Heavy Ion Transport code System, PHITS, version 2.52. *Journal of Nuclear Science and Technology* **50,** 913–923. eprint: http://dx.doi.org/10.1080/00223131.2013.814553. http://dx.doi.org/10.1080/00223131.2013.814553 (2013).
55. SHIBATA, K. *et al.* JENDL-4.0: A New Library for Nuclear Science and Engineering. *Journal of Nuclear Science and Technology* **48,** 1–30. eprint: https://doi.org/10.1080/18811248.2011.9711675. https://doi.org/10.1080/18811248.2011.9711675 (2011).
56. Hirayama, H., Namito, Y., Bielajew, A. F., Wilderman, S. J. & Nelson, W. The EGS5 code system. *KEK-2005-8, 38045743* (2005).
57. Nakao, N. *et al.* Measurements of response function of organic liquid scintillator for neutron energy range up to 135 MeV. *Nuclear Instruments and Methods in Physics Research Section A: Accelerators, Spectrometers, Detectors and Associated Equipment* **362,** 454–465. ISSN: 0168-9002. https://www.sciencedirect.com/science/article/pii/016890029500193X (1995).
58. Satoh, D. *et al. Study of light output and response function of liquid organic scintillator for high-energy neutron spectrometry* in *IEEE Nuclear Science Symposium Conference Record, 2005* **3** (2005), 1288–1290.
59. Mannhart, W. *Status of the Cf-252 fission neutron spectrum evaluation with regard to recent experiments* in (International Atomic Energy Agency, 1989), 305.
60. Couteur, K. J. L. *"The Statistical Model", in Nuclear Reactions, edited by P. M. Endt and M. Demeur, North Holland*
61. Ichimura, M., Sakata, F. & Matsuyanagi, K. *Theory of nucleus*
62. Hashim, I. H. *et al.* Muon capture reaction on ^{100}Mo to study the nuclear response for double-β decay and neutrinos of astrophysics origin. *Phys. Rev. C* **97,** 014617. https://link.aps.org/doi/10.1103/PhysRevC.97.014617 (1 2018).

63. Aichelin, J. "Quantum" molecular dynamics—a dynamical microscopic n-body approach to investigate fragment formation and the nuclear equation of state in heavy ion collisions. *Physics Reports* **202,** 233–360. ISSN: 0370-1573. https://www.sciencedirect.com/science/article/pii/0370157391900943 (1991).

64. Furihata, S., Koji, N., Meigo, S. & Ikeda Y. ad Maekawa, F. The GEM code A simulation program for the evaporation and the fission process of an excited nucleus. *JAERI-DATA/CODE–2001-015* (2001).

65. Schuster, P. F. *et al.* High resolution measurement of tagged two-neutron energy and angle correlations in ^{252}Cf (sf). *Phys. Rev. C* **100,** 014605. https://link.aps.org/doi/10.1103/PhysRevC.100.014605 (1 2019).

66. HANBURY BROWN, R. & TWISS, R. Q. A Test of a New Type of Stellar Interferometer on Sirius. *Nature* **178,** 1046–1048. https://doi.org/10.1038/1781046a0 (1956).

67. Ghetti, R. *et al.* Characterization of nuclear sources from neutron–neutron, proton–proton and neutron–proton correlation functions. *Nuclear Physics A* **674,** 277–297. ISSN: 0375-9474. https://www.sciencedirect.com/science/article/pii/S0375947400001561 (2000).

68. Colonna, N. *et al.* Measurement of Compound Nucleus Space-Time Extent with Two-Neutron Correlation Functions. *Phys. Rev. Lett.* **75,** 4190–4193. https://link.aps.org/doi/10.1103/PhysRevLett.75.4190 (23 1995).